

SHORT REPORT

Open Access



Effects of the *scid* mutation on X-ray-induced deletions in the brain and spleen of *gpt* delta mice

Kenichi Masumura^{1*}, Fumio Yatagai², Masako Ochiai^{3,4}, Hitoshi Nakagama^{3,5} and Takehiko Nohmi^{1*} 

Abstract

Background: DNA-dependent protein kinase (DNA-PK), consisting of a Ku heterodimer (Ku70/80) and a large catalytic subunit (DNA-PKcs), plays an important role in the repair of DNA double-strand breaks via non-homologous end-joining (NHEJ) in mammalian cells. Severe combined immunodeficient (*scid*) mice carry a mutation in the gene encoding DNA-PKcs and are sensitive to ionizing radiation. To examine the roles of DNA-PKcs in the generation of deletion mutations *in vivo*, we crossed *scid* mice with *gpt* delta transgenic mice for detecting mutations.

Results: The *scid* and wild-type (WT) *gpt* delta transgenic mice were irradiated with a single X-ray dose of 10 Gy, and Spi^- mutant frequencies (MFs) were determined in the brain and spleen 2 days after irradiation. Irradiation with X-rays significantly enhanced Spi^- MF in both organs in the *scid* and WT mice. The MFs in the brain of irradiated *scid* mice were significantly lower than those in WT mice, i.e., $2.9 \pm 1.0 \times 10^{-6}$ versus $5.0 \pm 1.1 \times 10^{-6}$ ($P < 0.001$), respectively. In the spleen, however, both mouse strains exhibited similar MFs, i.e., $4.1 \pm 1.8 \times 10^{-6}$ versus $4.8 \pm 1.4 \times 10^{-6}$. Unirradiated *scid* and WT mice did not exhibit significant differences in MFs in either organ.

Conclusions: DNA-PKcs is unessential for the induction of deletion mutations in the spleen, while it plays a role in this in the brain. Therefore, the contribution of DNA-PKcs to NHEJ may be organ-specific.

Keywords: DNA-PKcs, *scid* mice, Non-homologous end-joining, Spi^- assay, Deletion, X-irradiation

Introduction

The repair of DNA double-strand breaks (DSBs) is critical for the maintenance of genomic integrity. In mammalian cells, DSBs are repaired by the homologous recombination and/or the nonhomologous end-joining (NHEJ) pathways [1–3]. However, DSBs induced by ionizing radiation (IR) are mainly repaired through NHEJ pathway. This is particularly true in non-dividing cells and in G1 cells due to the absence of sister chromatids, the preferred substrate for homologous recombination. Although defects in NHEJ result in genomic

instability and cancer predisposition, NHEJ often leads to deletion mutations, with or without short length insertions, when DNA ends can't be directly ligated [4]. IR and chemical treatments usually induce modified DSBs with ends that are incompatible for direct ligation. Therefore, NHEJ can be regarded as a double-edged sword; while it prevents cell death and gross chromosome rearrangements, it often induces deletions and insertions during ligation of incompatible ends.

DNA-dependent protein kinase (DNA-PK) consists of three components, the catalytic subunit DNA-PKcs and the heterodimeric Ku70 and Ku80 proteins, and is involved in NHEJ of DNA DSBs and V(D)J recombination [5–9]. In general, when DNA DSBs are induced, Ku70/80 proteins bind to the ends and interact with other

* Correspondence: masumura@nihs.go.jp; nohmi@nihs.go.jp

¹Division of Genetics and Mutagenesis, National Institute of Health Sciences, 3-25-26 Tonomachi, Kawasaki-ku, Kawasaki-shi, Kanagawa 210-9501, Japan
Full list of author information is available at the end of the article



© The Author(s). 2020 **Open Access** This article is licensed under a Creative Commons Attribution 4.0 International License, which permits use, sharing, adaptation, distribution and reproduction in any medium or format, as long as you give appropriate credit to the original author(s) and the source, provide a link to the Creative Commons licence, and indicate if changes were made. The images or other third party material in this article are included in the article's Creative Commons licence, unless indicated otherwise in a credit line to the material. If material is not included in the article's Creative Commons licence and your intended use is not permitted by statutory regulation or exceeds the permitted use, you will need to obtain permission directly from the copyright holder. To view a copy of this licence, visit <http://creativecommons.org/licenses/by/4.0/>. The Creative Commons Public Domain Dedication waiver (<http://creativecommons.org/publicdomain/zero/1.0/>) applies to the data made available in this article, unless otherwise stated in a credit line to the data.

proteins including DNA PKcs and Artemis for end-resection, DNA polymerase μ and λ for addition of nucleotides, and the DNA ligase IV complex for ligation of the ends. However, different proteins are recruited to the site of DNA damage to participate in the repair of DSBs each time, depending on the end configurations i.e., blunt ends, 3'- or 5'-overhangs or ends containing modified bases [10].

The *scid* (severe combined immune-deficiency) mice bear a naturally occurring mutation in the DNA-PKcs gene that results in an 83-amino acid truncation of the C-terminal end [11–14]. These mice, and cells derived from them, are hypersensitive to IR, display defects in joining of IR-induced DNA DSBs [12, 15], and are defective in coding joint formation during V(D)J recombination [16, 17]. However, *scid* cells can form signal joints in V(D)J recombination [18], which involve the joining of the ends created after the excision of intervening DNA during V(D)J recombination and the formation of circular DNA molecules. In contrast, Ku-deficient mice and embryonic stem cells exhibit defects in both coding and signal joint formation [19–22]. Therefore, it appears that DNA-PKcs is only needed to resolve a subset of DSBs and that NHEJ may proceed in a DNA-PKcs-independent, as well as DNA-PKcs-dependent, manner.

We previously developed the *gpt* delta transgenic mouse for the detection of mutations in vivo [23–25]. In *gpt* delta mice, about 80 copies of lambda EG10 DNA, which carries *red* and *gam* genes, are integrated into each chromosome 17 in a C57BL/6J background [26, 27]. A feature of the mutation assay is its ability to efficiently detect certain types of deletions by Spi⁻ (sensitive to P2 interference) selection, as well as point mutations, i.e., base substitutions and frameshifts, by 6-thioguanine selection [28, 29]. Spi⁻ selection takes advantage of the restricted growth of the lambda phage in P2 lysogens [30]. Only mutant lambda phages that are deficient in the functions of both *red* and *gam* genes can grow well in P2 lysogens and display the Spi⁻ phenotype. Simultaneous inactivation of the two adjacent genes is usually induced by a deletion in the region, or frameshifts that interfere with the translation of both genes. Spi⁻ selection detects deletions ranging from single nucleotide (-1) frameshifts to 10 kb in size [29]. In this procedure, the lambda EG10 is rescued from the mouse genome by in vitro packaging reactions, and P2 lysogens are infected with the rescued phages to identify Spi⁻ plaque. We have demonstrated that the Spi⁻ mutant frequency (MF) is substantially increased by IR and chemical treatments, and suggested that NHEJ repair plays an important role in the induction of Spi⁻ deletion mutants [28, 31, 32].

Since NHEJ may proceed in DNA PKcs-dependent and independent manners, it may be possible that DNA

PKcs plays a significant role in deletion formation in one organ while it plays only a negligible role in another one. It is reported that MF of unirradiated *Ku80*^{-/-} mice is higher than that of WT mice in the spleen while the MFs are similar between two strains of mice in the liver [33]. To examine the possible variation of the roles of DNA PKcs in deletion mutations in mammalian organs, we crossed *scid* mice with *gpt* delta mice (hereafter, the offspring from this cross will be referred to as *scid* mice, and *gpt* delta mice as wild-type (WT) mice). We irradiated *scid* and WT mice with X-rays and compared Spi⁻ MFs in the brain and spleen, which are representative organs with quiescent and proliferating cells, respectively. The results indicated that X-ray irradiation significantly induced deletion mutations in both organs of *scid* and WT mice. Although *scid* mice exhibited significantly lower MFs than WT mice in the brain, both mouse strains exhibited similar MFs in the spleen. Possible mechanisms of DNA-PKcs-independent NHEJ of DNA DSBs are discussed.

Materials and methods

Treatment of animals

C.B-17 *scid* mice, maintained in CLEA Japan, were crossed with C57BL/6J lambda EG10-homozygous *gpt* delta mice [26]. The heterozygous F1 mice were mated with the same offspring carrying the *scid* mutation and lambda EG10 transgene, which resulted in F2 mice. The *scid* genotype of each experimental animal was confirmed by PCR, according to a previously reported method [13]. The existence of the transgene was also confirmed using a previously reported method [26]. Eleven- to twelve-week-old WT (*wt/wt*) and *scid* (*scid/scid*) mice were whole-body irradiated with X-rays; a total dose of 10 Gy. X ray-irradiation (200 kVp, Softex-Rigaku) was delivered at a dose rate of 1 Gy per min. Each group consisted of a total of 6–10 male and female mice. The mice were sacrificed 2 days following irradiation. The brain and spleen were collected and quickly frozen in liquid nitrogen and stored at -80 °C. Genomic DNA was extracted from the organs using the phenol/chloroform method and lambda EG10 phages were rescued using Transpack^R Packaging Extract (Agilent Technology, Japan) as described previously [24].

Spi⁻ mutation assay

The Spi⁻ mutation assay was performed as described previously [24]. The rescued phages were used to infect *E. coli* XL1-Blue MRA (P2) cells. The infected cells were mixed with molten soft agar, poured on lambda-trypticase agar plates, and incubated at 37 °C. The Spi⁻ candidate plaques detected on the plates were suspended in 50 μ L of SM buffer. The suspension was spotted on the plate where the XL1-Blue MRA (P2) cells were

spread. The plates were incubated at 37 °C; the mutants that produced clear spots were counted as confirmed Spi⁻ mutants. The rescued phages were also used to infect *E. coli* XL1-Blue MRA cells to determine the number of rescued phages. The Spi⁻ MF was calculated as described previously [24]. Phage lysates of the Spi⁻ mutants were used as templates for PCR analysis. The PCR primers were:

primer 001 (5'-CTCTCCTTTGATGCGAATGCCAG C-3'),

primer 002 (5'-GGAGTAATTATGCGGAACAGAAT CATGC-3'),

primer 005 (5'-CGTGGTCTGAGTGTGTTACAGAG G-3'),

primer 006 (5'-GTTATGCGTTGTTCCATACAACC TCC-3') and.

primer 012 (5'-CGGTGCGAGGGACCTAATAACTTC G-3').

The appropriate primers for DNA sequencing were selected based on the results of PCR analysis. The sequencing primers have been described previously [34–36]. The entire sequence of lambda EG10 is available at <http://www.nih.gov/jp/dgm/dgm3/eg10v20.txt>. DNA sequencing was performed with BigDye™ Terminator Cycle Sequencing Kit (Applied Biosystems, Foster City, CA) and ABI PRISM™ 310 Genetic Analyzer (Applied Biosystems).

Statistical analysis

All data were expressed as mean ± standard deviation (SD). A Tukey-test was used to determine if the differences between two groups were statistically significant. A *P* value of <0.05 was considered statistically significant.

Results

Spi⁻ MFs in the brain and spleen of X-ray-irradiated mice

WT and *scid* mice were exposed to X-ray irradiation at a dose of 10 Gy and Spi⁻ MFs were determined in the brain and spleen (Fig. 1, Supplementary Table 1 and 2). X-ray irradiation significantly enhanced Spi⁻ MFs in both organs in WT and *scid* mice. The MFs in the brain of *scid* mice were significantly lower than those of WT mice, i.e., $2.9 \pm 1.0 \times 10^{-6}$ versus $5.0 \pm 1.1 \times 10^{-6}$, *P* < 0.001. In the spleen, however, both mouse strains exhibited similar MFs after irradiation ($4.1 \pm 1.8 \times 10^{-6}$ vs $4.8 \pm 1.4 \times 10^{-6}$, *P* = 0.77). Unirradiated *scid* and WT mice did not exhibit significant differences in MFs in either organ ($0.85 \pm 0.67 \times 10^{-6}$ vs $1.0 \pm 0.64 \times 10^{-6}$ in the brain and $1.4 \pm 0.31 \times 10^{-6}$ vs $2.6 \pm 1.3 \times 10^{-6}$ in the spleen).

Deletion mutation spectra in the brain of WT and *scid* mice

Since MFs in the brain were significantly lower in *scid* mice than in WT mice, we were interested in whether the spectra of deletions were different in the two strains of mice. Therefore, we sequenced the Spi⁻ mutants recovered from the brain of X-ray-irradiated and unirradiated WT and *scid* mice (Tables 1 and 2). The specific MFs of each type of deletion were calculated by multiplying the MF by the ratio of the number of each class of mutations to the total number of deletion mutations.

In WT mice, the frequency of 1 base pair (bp)-deletions increased 3.0-fold by irradiation (0.82 to 2.50×10^{-6}), while the frequency of deletions of more than 2 bps in size, increased 20.3-fold (0.12 to 2.43×10^{-6}). Among the sequenced 35 deletions of more than 2 bps in size, 37% (13/35) were deletions of more than 1 kb and 60% (21/35) had microhomologous sequences of 1

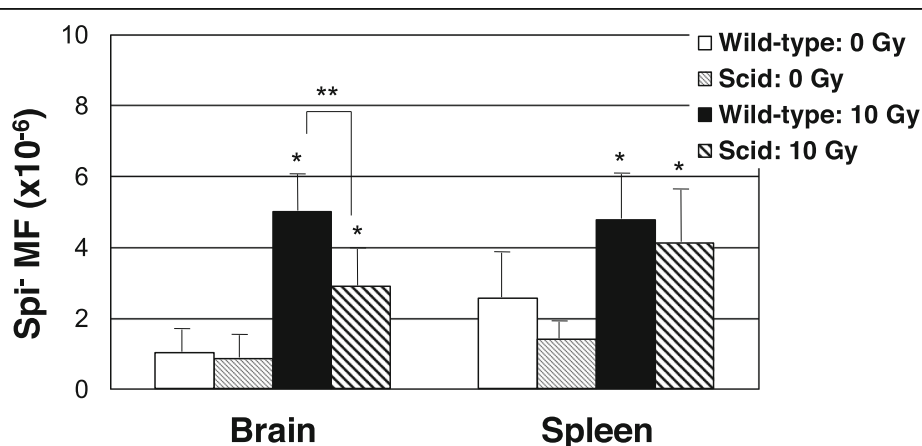


Fig. 1 The Spi⁻ MFs in the brain and the spleen of WT and *scid* mice with or without X-ray-irradiation. Error bars mean ± SD of the MFs in each group; *n* = 10 for WT (0 Gy), *n* = 8 for WT (10 Gy), *n* = 6 for *scid* (0 Gy) and *n* = 7 for *scid* (10 Gy). * *P* < 0.01, relative to the unirradiated groups. ** *P* < 0.01, relative to the WT mice. A Tukey-test was used to determine if the differences between two groups were statistically significant

Table 1 Spi⁻ mutation spectra in the brain of X-ray-irradiated WT and the *scid* mice

	WT 0 Gy			WT 10 Gy			<i>scid</i> 0 Gy			<i>scid</i> 10 Gy		
	No.	%	MFx10 ⁻⁶	No.	%	MFx10 ⁻⁶	No.	%	MFx10 ⁻⁶	No.	%	MFx10 ⁻⁶
1 bp deletion												
In run	18	72	0.74	30	42	2.08	6	75	0.64	40	42	1.22
Other	2	8	0.08	6	8	0.42	0	0	0.00	10	11	0.30
> 2 bp deletion												
With microhomology	0	0	0.00	21	29	1.46	0	0	0.00	25	26	0.76
Without microhomology	3	12	0.12	12	17	0.83	1	13	0.11	11	12	0.33
Insertion	0	0	0.00	2	3	0.14	0	0	0.00	4	4	0.12
Insertion	2	8	0.08	0	0	0.00	0	0	0.00	5	5	0.15
Complex	0	0	0.00	1	1	0.07	1	13	0.11	0	0	0.00
Total	25	100	1.03	72	100	5.00	8	100	0.85	95	100	2.89

Specific MFs were calculated by multiplying the total MF by the ratio of each class of mutants

In unirradiated WT mice, total 26 mutants (suppl. Table 1) were obtained. They were sequenced and 25 deletion mutations (Table 1) were identified. In 10 Gy-irradiated WT mice, total 172 mutants were obtained. Eighty seven mutants were sequenced and 72 deletion mutations were identified. In unirradiated *scid* mice, total 9 mutants were obtained. All were sequenced and 8 deletion mutations were identified. In 10 Gy-irradiated *scid* mice, total 67 + 89 mutants were obtained. One hundred and twenty five were sequenced and 95 deletion mutations were identified. In 10 Gy-irradiated *scid* mice, 89 mutants were obtained by additional plating for sequencing analysis, but they were not used for calculation of MF because no additional plating was conducted for control groups

to 4 bps at the junction. The average length of microhomology was 1.8 bp. Six % (2/35) had an inserted base at the junctions.

In *scid* mice, the frequency of 1 bp-deletions increased 2.4-fold by irradiation (0.64 to 1.52×10^{-6}), while the frequency of deletions of more than 2 bps in size, increased 11.1-fold (0.11 to 1.22×10^{-6}). Among the sequenced 40 deletions of more than 2 bps in size, 35% (14/40) were more than 1 kb and 63% (25/40) had microhomologous sequences at the junction. With the exception of one mutation that had a 12-bp microhomology, the average length of microhomology was 1.7 bp. Five mutations containing a 1 bp-insertion, not accompanied by deletions, were observed in irradiated *scid* mice, whereas no such mutations were observed in irradiated WT mice.

There was no significant difference in the mutation spectra between unirradiated WT and *scid* mice. One bp-deletions in the repetitive sequences were the most dominant type of mutation. Three hotspots were observed in unirradiated mice: 1) AAAAA to AAAA at position 227–231, 2) GGGG to GGG at position 286–289 and 3) AAAAAA to AAAAA at position 295–300 in the *gam* gene.

Discussion

Although it is well known that the *scid* mice are severely sensitive to killing effects of irradiation, little is known about the roles of DNA PKcs in irradiation-induced deletion mutations in various organs of mice. In this study, the WT and *scid* mice were irradiated with X-rays and deletion mutations were analyzed in the brain and the spleen. In the X-ray-irradiated WT mice, the Spi⁻ MFs

in the brain and spleen were significantly higher than those of unirradiated mice. Sequencing analysis of the Spi⁻ mutants in the brain showed that X-ray irradiation preferentially induced large deletions of up to 10 kbps (Table 1). Specific MFs of deletions of more than 2 bps in size increased 20.3-fold upon irradiation, in contrast to the MFs of deletions of 1 bp that increased 3.0-fold. Among the sequenced 35 deletions of more than 2 bps in size, 60% (21/35) had microhomologous sequences of 1–4 bps at the deleted junction (Table 2). These data confirmed that deletions of more than 2 bps in size in this study are largely generated through NHEJ of DNA DSBs [3, 29].

In irradiated *scid* mice, the Spi⁻ MFs were significantly increased 3.2- and 2.9-fold in the brain and spleen, respectively, compared with those of unirradiated *scid* mice. In the brain, the specific MF of deletions of more than 2 bps in size increased 11-fold by irradiation, in contrast to the MF of 1 bp-deletions that increased 1.9-fold (Table 1). Sequencing analysis of the Spi⁻ mutants showed that 63% (25/40) of the deletions of more than 2 bps in size had microhomologous sequences of 1–12 bps at the deleted junction. These characteristics of the X-ray-induced deletions in *scid* mice were similar to those of WT mice, suggesting that X-ray-induced DSBs are repaired by NHEJ even without DNA-PKcs. It is possible, however, that the defective protein encoded by the murine *scid* allele retains enough residual function to support NHEJ. Bogue et al. examined V(D)J recombination in DNA-PKcs-deficient SLIP mice and found that the effects of this mutation on coding and signal joint formation are identical to the effects of the *scid* mutation [18]. These data are incompatible with the notion

Table 2 Summary of Spi⁻ mutations in the brain of X-ray-irradiated WT and *scid* mice

Types of deletions	Position in <i>gam</i>	Position in lambda EG10	Sequence Change ^a	Sequence at junction ^{b,c}	No. of mutants			
					WT	<i>scid</i>	WT	<i>scid</i>
					0 Gy	0 Gy	10 Gy	10 Gy
One base pair deletions								
In run sequences								
	141–142		GG→G				1	
	188–190		CCC→CC					1
	199–201		AAA→AA				1	
	227–231		AAAAA→AAAA		5 ^d	1	5 ^d	11 ^d
	238–241		CCCC→CCC		2 ^d	1	1	2 ^d
	286–289		GGGG→GGG		5 ^d	1	3 ^d	12 ^d
	290–291		CC→C				1	1
	295–300		AAAAAA→AAAAA		6 ^d	3 ^d	15 ^d	9 ^d
	316–318		TTT→TT				1	
	334–336		TTT→TT					2
	377–378		CC→C					1
	380–381		TT→T				1	
	387–388		CC→C				1	
	390–391		CC→C					1
Other 1 bp deletion								
	131		ttAtt→tttt					1
	175		cacTAc→cacac					1
	183		caGct→cact					1
	203		gAgg→ggg					1
	218		agAcg→agcg		1			
	236		ccTgc→ccgc					1
	268		tcGat→tcat				1	
	276		tttG→ttt				1	
	277		ttgCaac→ttgaac					2 ^d
	285		Cgggg→ggggg				1	
	294		Caaaaaa→aaaaaa		1			
	301		aaaaaaT→aaaaaa					1
	320		tttgAt→tttgt					1
	328		tGtt→ttt					1
	332		gAg→gg				1	
	341		ggAg→ggg				1	
	392		ccAgg→ccgg					1
> 2 bp deletions								
Deleted sizes (bp)								
2	153 → 156			tgag tcag			1	
2	251 → 254			tggt aatc				1
2	349 → 352			atgg gaac			1	
3	355 → 359			gaac tccg				1
4	182–184 →			agcaGCcgt			1	

Table 2 Summary of Spi⁻ mutations in the brain of X-ray-irradiated WT and *scid* mice (Continued)

Types of deletions	Position in <i>gam</i>	Position in lambda EG10	Sequence Change ^a	Sequence at junction ^{b,c}	No. of mutants			
					WT	<i>scid</i>	WT	<i>scid</i>
					0 Gy	0 Gy	10 Gy	10 Gy
	187–189							
4	222 → 227			cgac aaaa				1
4	239–240 → 244–245			tgcc C acct				1
4	247–249 → 251–253			cacc T gaat			1	
4	295–300			cagc AA tcca				1
4	304 → 309			tcca ccgt				1
5	300–301 → 306–307			aaaa T accc				2
7	147–149 → 155–157			tcgt CT caga				1
7	349–351 → 357–359			atgg CA tccg			1	
8	175 → 184			cact ctcg			1	
10	196–198 → 207–209			gaag AG gaact			1	
10	323 → 334			atga tttc			1	
10	335 → 346			agtt atgg			1	
10	375–379 → 386–390			tgaa AC cacc			1	
12	221–222 → 234–235			acga C ctgc				1
12	313 → 326			cgtg atgt			1	
13	376–379 → 389–392			gaaa CC Aggtt			1	
14	165–167 → 180–182			ctgg G cagc			1	
17	154–155 → 172–173			gagg C acta			1	
17	239–240 → 257–258			ctgc C gcta				1
17	251 → 269			tgtt atca				1
19	212–215 → 232–235			aact GGC ctgc				1
22	288–289 → 311–312			cggg G tgcg				3
26	268 → 285			atcg cggg				2 ^d
28	307 → 336			atta tcag			1	
28	338 → 367			ttca atgg		1		
32	189–190 → 222–223			cgcc C atgg			1	
34	346–348 → 381–383			cgca TG ctca			1	
41	380 → 422			ccat aatg				1
49	206 → 257 (1 bp ins.)			aggc C cgct			1	
67	246–247 →			gcac C gttt				1

Table 2 Summary of Spi⁻ mutations in the brain of X-ray-irradiated WT and *scid* mice (Continued)

Types of deletions	Position in <i>gam</i>	Position in lambda EG10	Sequence Change ^a	Sequence at junction ^{b,c}	No. of mutants			
					WT	<i>scid</i>	WT	<i>scid</i>
					0 Gy	0 Gy	10 Gy	10 Gy
	314–315							
76	189 → 266			cgcc tcga			1	
86	252–253 → 339–340			gttt G gagc			1	
107	91–92 → 199–200			cgat A aaga			1	
124	208 → 333			gcag gttt				1
127	273–276 → 401–404			tcatt TTG attc				1
151		24,867–24,870 → 25,019–25,022		cgac ACG cacg			1	
432		24,828–24,830 → 25,261–25,263		gagt GG gctg				1
449		24,683–24,684 → 25,133–25,134		ccca C tttc				1
596		24,446–24,450 → 25,043–25,047		ata TGGC ccccg				1
654		24,719 → 25,374		aagg tcgc				1
1248		24,524–24,536 → 25,767–25,779		aatg GTTGCGGCGGC gtg				2
1436		24,563 → 26,000		caga cagt		1		
1557		24,222 → 25,802 (22 bps ins.)		tgtc CATTCAAACACAC CACCAAAG ctcc				1
1616		23,938–25,555 (2 bps ins.)		aaac AG gcct			1	
1856		23,960–23,961 → 25,817–25,818		gaag T tggt			1	
1874		24,161–24,162 → 26,009–26,010		tggt T gctg			1	
2124		23,141 → 25,266 (1 bp ins.)		tcgg A gatt				2
2388		23,000–23,004 → 25,389–25,393		tgct GCGA tag				1
2388		24,000–24,002 → 28,232–28,234		ggg GT gtca				1
2441		24,034–24,035 → 26,476–26,477		cggt G ccag				1
2842		24,247–24,248 → 27,090–27,091		agc G ccga				1
3628		25,062 → 28,691		aaa ctg			1	
3701		24,560 → 28,262		gatg gcac				1
3707		21,458–21,459 → 25,166–25,167		att G cgcc				1
3979		22,200–22,204 → 26,180–26,184		ccag TTTA tttt			2	
4144		22,585–22,586 → 26,730–26,731		cgtt C tgcc				1
4689		23,611–23,612 → 28,301–28,302		agtt G cgcg			1	
4698		24,423–24,424 → 29,122–29,123		gaa G tgcc				1
4841		21,691–21,692 → 26,533–26,534		agac A tcatt			1	
5037		21,355 → 26,393		ctct agaa			1	
5251		19,712–19,713 → 24,964–24,965		cacc A ccatt			1	
5422		22,340 → 27,760 (3 bps ins.)		cgcc TTT caca				1
5562		19,997 → 25,560		atag gatt		1		
5727		19,335 → 25,063		tggc tgat			1	
6900		24,036 → 30,937		gtga gatc			1	
7303		23,917 → 31,221		cttc tcgt		1		
9030		21,854–21,857 → 30,885–30,888		gagt ACG cttt				1

Table 2 Summary of Spi⁻ mutations in the brain of X-ray-irradiated WT and *scid* mice (Continued)

Types of deletions	Position in <i>gam</i>	Position in lambda EG10	Sequence Change ^a	Sequence at junction ^{b,c}	No. of mutants			
					WT	<i>scid</i>	WT	<i>scid</i>
					0 Gy	0 Gy	10 Gy	10 Gy
Insertions								
+ 1	227–231		AAAAA→AAAAAA		1			
+ 1	227–231		AAAAA→AAAAAA					1
+ 1	295–300		AAAAAA→AAAAAAA					4 ^d
+ 1	356		aaca→aacTa		1			
Complex								
N.D.		23,999 → 24,381, 23,997–23,996 → 27,762–27,763				1		
N.D.		21,108–21,109 → 13–14						1
					25	8	72	95

^a Capital letters are deleted or inserted bases

^b Bold and underlined bases denote homologous sequences of deletion junctions

^c Bold and italic bases denote inserted sequences at deletion junctions

^d The mutations were independently observed from more than two different mice

that signal joint formation in *scid* mice results from residual DNA-PKcs function and support the idea that DNA-PKcs is not an essential factor for NHEJ in mice. The analysis of DNA-PKcs knock-out mice also supports this idea [37]. Hence, we suggest that DNA-PKcs-independent NHEJ is responsible for deletions associated with X-ray exposure in the spleen and, in part, in the brain.

How can NHEJ proceed without DNA-PKcs in the brain and spleen? DNA-PKcs interacts with the C-terminal part of Ku80, a component of DNA-PK. When Ku binds to DNA ends, the interaction with DNA PKcs increases substantially, which leads to autophosphorylation of DNA PKcs and activation of the endonuclease activities of Artemis [38]. This endonuclease appears to play a role in the removal of 5'- and 3'-overhangs in DNA ends, which seems to be a necessary step for the efficient ligation of broken DNA ends. It is estimated, however, that more than half of IR-induced DSBs are repaired even without the activities of Artemis [39, 40]. This suggests that nucleases other than Artemis, such as Apratoxin and PNKP-like factor (APLF), flap endonuclease (FEN1), DNA replication helicase/nuclease 2 (DNA 2) and exonuclease 1, may play roles in the resection of broken DNA with incompatible DNA ends [3]. We speculate, therefore, that DNA PKcs-independent nucleases may play roles in NHEJ in the brain and spleen while the canonical DNA PKcs-dependent Artemis is involved in NHEJ in the brain. Obviously, further work is needed to reveal exact mechanisms by which NHEJ proceeds without DNA PKcs in the organs.

Unirradiated *scid* and WT mice did not exhibit significant differences in MFs in the brain and spleen (Fig. 1). In addition, the spectra of deletions were similar

between the two strains of mice, where 1 bp-deletions in the repetitive sequences were the most dominant. These deletions, however, are mostly generated by slippage of DNA polymerases during DNA replication and not during DNA repair of DSBs [29]. It is reported that spontaneous *lacI* MFs were similar between *scid* and WT mice in the brain, spleen and liver [41]. Spontaneous MF of expanded simple tandem repeat (ESTR) in male germline was higher in the *scid* mice than in the WT mice although the frequency was not enhanced by irradiation [42].

Lee et al. report that DNA-PK activity fluctuates in a cell cycle-dependent manner, and propose a model in which two illegitimate recombinational repair pathways exist in mammals, one of them being DNA-PK dependent and restricted to the G1/early S phase and the other being DNA-PK independent and restricted to the late S/G2 phase of the cell cycle [43]. They showed that the DNA DSB repair activity in the *scid* pre-B cells was greatly reduced during the G1/early S phase resulting in increased X-ray hypersensitivity but was indistinguishable from that in WT cells during the late S and G2 phases. In the spleen, in which cell division is active, DNA-PK independent repair may work well during the late S and G2 phases and neutralize the effect of the *scid* mutation. In the brain, in which cell division is inactive, DNA-PK dependent end-joining may play an important role in DSB repair and, in this context, the *scid* mutation may lead to a reduced activity of DSB repair and the induction of deletion mutations. In the mutation spectra of Spi⁻ mutations recovered from the brain of the irradiated *scid* mice, there were 4 mutations having insertion sequences at the deleted junctions and 5 mutations having + 1 insertions. This was observed in 9.5% (9/95)

of the analyzed samples (Table 2). In the irradiated WT mice, there were 2 mutations having insertion sequences at the deleted junctions and no mutations having +1 insertions. This was observed in 2.8% (2/72) of the analyzed samples. The higher frequency of mutations with insertions that was observed in the irradiated *scid* mice raises the possibility that DNA-PKcs-independent NHEJ may incorporate more nucleotides compared with DNA-PKcs-dependent NHEJ during DNA DSBs repair. Other characteristics of the mutation spectra in the brain of irradiated mice were similar between *scid* and WT mice.

Conclusions

X-ray-induced deletions are predominantly generated by NHEJ in the brain and spleen of irradiated mice. NHEJ proceeds in DNA-PKcs-dependent and DNA PKcs-independent manners. DNA-PKcs contributes to NHEJ in the brain while it is dispensable in the spleen. This study suggests the organ specificity of the roles of DNA PKcs in deletion induction and raises a question of how NHEJ proceeds in the absence of DNA PKcs in mammalian organs.

Supplementary information

Supplementary information accompanies this paper at <https://doi.org/10.1186/s41021-020-00158-y>.

Additional file 1: Table S1. Spi⁻ mutant frequency in the brain of X-ray-irradiated mice. **Table S2.** Spi⁻ mutant frequency in the spleen of X-ray-irradiated mice.

Abbreviations

DNA-PK: DNA-dependent protein kinase; DNA PKcs: The catalytic subunit of DNA PK; *scid*: Severe combined immunodeficient; WT: Wild type; MFs: Mutant frequencies; NHEJ: Non-homologous end-joining; DSBs: Double-strand breaks; IR: Ionizing radiation; Spi: Sensitive to P2 interference; SD: Standard deviation; bp: Base pair; APLF: Apratoxin and PNKP-like factor; FEN1: Flap endonuclease; DNA 2: DNA replication helicase/nuclease 2; ESTR: Expanded simple tandem repeat

Acknowledgements

We acknowledge Ms. Makiko Hoshino, Showa Pharmaceutical University, for technical assistance for mutant analyses. We thank Drs. Otoyua Ueda and Hiroshi Suzuki, Exploratory Research Laboratory, Fuji Gotemba Research Laboratory, Chugai Pharmaceutical Co., Ltd., for generation of the *scid/gpt* delta mice.

Authors' contributions

MK and TN designed the experiments and MK conducted most of the experiments. FY irradiated the mice with X-ray and MO and HN characterized the *scid* mice. TN wrote the draft and all the authors confirmed the final manuscript.

Funding

This study was financially supported by the budget for Nuclear Research of the Ministry of Education, Culture, Sports, Science and Technology, Japan, based on the screening and counselling by the Atomic Energy Commission. This work was also supported by the Japan Health Science Foundation and the Tsuchikawa Memorial Fund for Study in Mammalian Mutagenicity.

Availability of data and materials

All data generated or analysed during this study are included in this published article and its Supplementary Table 1 and 2.

Ethics approval and consent to participate

All animal care and experimental procedures were conducted in compliance with the internal regulation for animal use at the National Institute of Health Sciences.

Consent for publication

Not applicable.

Competing interests

The authors declare that they have no competing interests.

Author details

¹Division of Genetics and Mutagenesis, National Institute of Health Sciences, 3-25-26 Tonomachi, Kawasaki-ku, Kawasaki-shi, Kanagawa 210-9501, Japan.

²Center for Sustainable Resource Science, The Institute of Physical and Chemical Research, 2-1 Hirosawa, Wako-shi, Saitama 351-0198, Japan.

³Biochemistry Division, National Cancer Center Research Institute, 5-1-1 Tsukiji, Chuo-ku, Tokyo 104-0045, Japan. ⁴Present Address: Department of Animal Experimentation, National Cancer Center Research Institute, 5-1-1 Tsukiji, Chuo-ku, Tokyo 104-0045, Japan. ⁵Present Address: National Cancer Center, 5-1-1 Tsukiji, Chuo-ku, Tokyo 104-0045, Japan.

Received: 7 February 2020 Accepted: 16 May 2020

Published online: 24 May 2020

References

- Jackson SP. Sensing and repairing DNA double-strand breaks. *Carcinogenesis*. 2002;23(5):687–96.
- Takata M, Sasaki MS, Sonoda E, Morrison C, Hashimoto M, Utsumi H, et al. Homologous recombination and non-homologous end-joining pathways of DNA double-strand break repair have overlapping roles in the maintenance of chromosomal integrity in vertebrate cells. *EMBO J*. 1998;17(18):5497–508.
- Pannunzio NR, Watanabe G, Lieber MR. Nonhomologous DNA end-joining for repair of DNA double-strand breaks. *J Biol Chem*. 2018;293(27):10512–23.
- Seol JH, Shim EY, Lee SE. Microhomology-mediated end joining: good, bad and ugly. *Mutat Res*. 2018;809:81–7.
- Jeggo PA, Taccioli GE, Jackson SP. Menage a trois: double strand break repair, V(D)J recombination and DNA-PK. *Bioessays*. 1995;17(11):949–57.
- Hefferin ML, Tomkinson AE. Mechanism of DNA double-strand break repair by non-homologous end joining. *DNA Repair (Amst)*. 2005;4(6):639–48.
- Smith GC, Jackson SP. The DNA-dependent protein kinase. *Genes Dev*. 1999;13(8):916–34.
- Collis SJ, DeWeese TL, Jeggo PA, Parker AR. The life and death of DNA-PK. *Oncogene*. 2005;24(6):949–61.
- Davis AJ, Chen BP, Chen DJ. DNA-PK: a dynamic enzyme in a versatile DSB repair pathway. *DNA Repair (Amst)*. 2014;17:21–9.
- Chang HH, Watanabe G, Gerodimos CA, Ochi T, Blundell TL, Jackson SP, et al. Different DNA end configurations dictate which NHEJ components are most important for joining efficiency. *J Biol Chem*. 2016;291(47):24377–89.
- Kirchgessner CU, Patil CK, Evans JW, Cuomo CA, Fried LM, Carter T, et al. DNA-dependent kinase (p350) as a candidate gene for the murine SCID defect. *Science*. 1995;267(5201):1178–83.
- Finnie NJ, Gottlieb TM, Blunt T, Jeggo PA, Jackson SP. DNA-dependent protein kinase activity is absent in *xrs-6* cells: implications for site-specific recombination and DNA double-strand break repair. *Proc Natl Acad Sci U S A*. 1995;92(1):320–4.
- Blunt T, Gell D, Fox M, Taccioli GE, Lehmann AR, Jackson SP, et al. Identification of a nonsense mutation in the carboxyl-terminal region of DNA-dependent protein kinase catalytic subunit in the *scid* mouse. *Proc Natl Acad Sci U S A*. 1996;93(19):10285–90.
- Araki R, Fujimori A, Hamatani K, Mita K, Saito T, Mori M, et al. Nonsense mutation at Tyr-4046 in the DNA-dependent protein kinase catalytic subunit of severe combined immune deficiency mice. *Proc Natl Acad Sci U S A*. 1997;94(6):2438–43.
- Biedermann KA, Sun JR, Giaccia AJ, Tosto LM, Brown JM. *scid* mutation in mice confers hypersensitivity to ionizing radiation and a deficiency in DNA double-strand break repair. *Proc Natl Acad Sci U S A*. 1991;88(4):1394–7.

16. Schuler W, Weiler U, Schuler A, Phillips RA, Rosenberg N, Mak TW, et al. Rearrangement of antigen receptor genes is defective in mice with severe combined immune deficiency. *Cell*. 1986;46(7):963–72.
17. Bosma MJ, Carroll AM. The SCID mouse mutant: definition, characterization, and potential uses. *Annu Rev Immunol*. 1991;9:323–50.
18. Bogue MA, Jhappan C, Roth DB. Analysis of variable (diversity) joining recombination in DNA-dependent protein kinase (DNA-PK)-deficient mice reveals DNA-PK-independent pathways for both signal and coding joint formation. *Proc Natl Acad Sci U S A*. 1998;95(26):15559–64.
19. Nussenzweig A, Chen C, da Costa Soares V, Sanchez M, Sokol K, Nussenzweig MC, et al. Requirement for Ku80 in growth and immunoglobulin V(D)J recombination. *Nature*. 1996;382(6591):551–5.
20. Zhu C, Bogue MA, Lim DS, Hasty P, Roth DB. Ku86-deficient mice exhibit severe combined immunodeficiency and defective processing of V(D)J recombination intermediates. *Cell*. 1996;86(3):379–89.
21. Gu Y, Seidl KJ, Rathbun GA, Zhu C, Manis JP, van der Stoep N, et al. Growth retardation and leaky SCID phenotype of Ku70-deficient mice. *Immunity*. 1997;7(5):653–65.
22. Li GC, Ouyang H, Li X, Nagasawa H, Little JB, Chen DJ, et al. Ku70: a candidate tumor suppressor gene for murine T cell lymphoma. *Mol Cell*. 1998;2(1):1–8.
23. Nohmi T, Katoh M, Suzuki H, Matsui M, Yamada M, Watanabe M, et al. A new transgenic mouse mutagenesis test system using Spi⁻ and 6-thioguanine selections. *Environ Mol Mutagen*. 1996;28(4):465–70.
24. Nohmi T, Suzuki T, Masumura K. Recent advances in the protocols of transgenic mouse mutation assays. *Mutat Res*. 2000;455(1–2):191–215.
25. Aoki Y, Nakajima D, Matsumoto M, Yagishita M, Matsumoto M, Yanagisawa R, et al. Change over time of the mutagenicity in the lungs of *gpt* delta transgenic mice by extract of airborne particles collected from ambient air in the Tokyo metropolitan area. *Genes Environ*. 2018;40:25.
26. Masumura K, Matsui M, Katoh M, Horiya N, Ueda O, Tanabe H, et al. Spectra of *gpt* mutations in ethylnitrosourea-treated and untreated transgenic mice. *Environ Mol Mutagen*. 1999;34(1):1–8.
27. Masumura K, Sakamoto Y, Kumita W, Honma M, Nishikawa A, Nohmi T. Genomic integration of lambda EG10 transgene in *gpt* delta transgenic rodents. *Genes Environ*. 2015;37:24.
28. Nohmi T, Suzuki M, Masumura K, Yamada M, Matsui K, Ueda O, et al. Spi⁻ selection: an efficient method to detect gamma-ray-induced deletions in transgenic mice. *Environ Mol Mutagen*. 1999;34(1):9–15.
29. Nohmi T, Masumura K. Molecular nature of intrachromosomal deletions and base substitutions induced by environmental mutagens. *Environ Mol Mutagen*. 2005;45(2–3):150–61.
30. Ikeda H, Shimizu H, Ukita T, Kumagai M. A novel assay for illegitimate recombination in *Escherichia coli*: stimulation of lambda bio transducing phage formation by ultra-violet light and its independence from RecA function. *Adv Biophys*. 1995;31:197–208.
31. Takeiri A, Mishima M, Tanaka K, Shioda A, Ueda O, Suzuki H, et al. Molecular characterization of mitomycin C-induced large deletions and tandem-base substitutions in the bone marrow of *gpt* delta transgenic mice. *Chem Res Toxicol*. 2003;16(2):171–9.
32. Nohmi T, Masumura K. *gpt* delta transgenic mouse: a novel approach for molecular dissection of deletion mutations in vivo. *Adv Biophys*. 2004;38:97–121.
33. Busuttill RA, Munoz DP, Garcia AM, Rodier F, Kim WH, Suh Y, et al. Effect of Ku80 deficiency on mutation frequencies and spectra at a *LacZ* reporter locus in mouse tissues and cells. *PLoS One*. 2008;3(10):e3458.
34. Horiguchi M, Masumura K, Ikehata H, Ono T, Kanke Y, Nohmi T. Molecular nature of ultraviolet B light-induced deletions in the murine epidermis. *Cancer Res*. 2001;61(10):3913–8.
35. Yatagai F, Kurobe T, Nohmi T, Masumura K, Tsukada T, Yamaguchi H, et al. Heavy-ion-induced mutations in the *gpt* delta transgenic mouse: effect of *p53* gene knockout. *Environ Mol Mutagen*. 2002;40(3):216–25.
36. Masumura K, Kuniya K, Kurobe T, Fukuoka M, Yatagai F, Nohmi T. Heavy-ion-induced mutations in the *gpt* delta transgenic mouse: comparison of mutation spectra induced by heavy-ion, X-ray, and gamma-ray radiation. *Environ Mol Mutagen*. 2002;40(3):207–15.
37. Gao Y, Chaudhuri J, Zhu C, Davidson L, Weaver DT, Alt FW. A targeted DNA-PKcs-null mutation reveals DNA-PK-independent functions for KU in V(D)J recombination. *Immunity*. 1998;9(3):367–76.
38. Ma Y, Pannicke U, Schwarz K, Lieber MR. Hairpin opening and overhang processing by an Artemis/DNA-dependent protein kinase complex in nonhomologous end joining and V(D)J recombination. *Cell*. 2002;108(6):781–94.
39. Riballo E, Kuhne M, Rief N, Doherty A, Smith GC, Recio MJ, et al. A pathway of double-strand break rejoining dependent upon ATM, Artemis, and proteins locating to gamma-H2AX foci. *Mol Cell*. 2004;16(5):715–24.
40. Kurosawa A, Koyama H, Takayama S, Miki K, Ayusawa D, Fujii M, et al. The requirement of Artemis in double-strand break repair depends on the type of DNA damage. *DNA Cell Biol*. 2008;27(1):55–61.
41. Andrew SE, Pownall S, Fox J, Hsiao L, Hambleton J, Penney JE, et al. A novel lacI transgenic mutation-detection system and its application to establish baseline mutation frequencies in the scid mouse. *Mutat Res*. 1996;357(1–2):57–66.
42. Yamauchi M, Nishimura M, Tsuji S, Terada M, Sasanuma M, Shimada Y. Effect of SCID mutation on the occurrence of mouse Pc-1 (Ms6-hm) germline mutations. *Mutat Res*. 2002;503(1–2):43–9.
43. Lee SE, Mitchell RA, Cheng A, Hendrickson EA. Evidence for DNA-PK-dependent and -independent DNA double-strand break repair pathways in mammalian cells as a function of the cell cycle. *Mol Cell Biol*. 1997;17(3):1425–33.

Publisher's Note

Springer Nature remains neutral with regard to jurisdictional claims in published maps and institutional affiliations.

Ready to submit your research? Choose BMC and benefit from:

- fast, convenient online submission
- thorough peer review by experienced researchers in your field
- rapid publication on acceptance
- support for research data, including large and complex data types
- gold Open Access which fosters wider collaboration and increased citations
- maximum visibility for your research: over 100M website views per year

At BMC, research is always in progress.

Learn more biomedcentral.com/submissions

